

Kramer-Pesch effect and damping of the vortex motion in the cuprate superconductors

S. G. Doettinger, R. P. Huebener, and S. Kittelberger

Physikalisches Institut, Lehrstuhl Experimentalphysik II, Universität Tübingen, Morgenstelle 14, D-72076 Tübingen, Germany

(Received 9 September 1996)

Kramer and Pesch discussed the fact that in the clean limit the radius of a vortex core in a type-II superconductor decreases proportionally to T with decreasing temperature. This ‘‘Kramer-Pesch effect’’ results from the thermal population of the quasiparticle bound states in the vortex core. In addition to the case of a static vortex, this effect also has important consequences for the vortex dynamics. Because of this, for the cuprate superconductors features of the damping of the vortex motion are expected at low temperatures. We discuss recent measurements of the electric resistance at high vortex velocities and of the microwave power absorption for different cuprate superconductors in conjunction with the Kramer-Pesch effect. [S0163-1829(97)01309-X]

I. INTRODUCTION

About 20 years ago, Kramer and Pesch discussed the spatial structure of a vortex in a type-II superconductor in the clean limit and for s -wave symmetry of the order parameter.^{1,2} They showed that the order parameter and the supercurrent density increase with increasing radial distance from the vortex center over a length scale $\xi_1 = \xi_{\text{BCS}}(T/T_c)$. Here, ξ_{BCS} is the BCS coherence length. This peculiar behavior, namely the shrinking of the vortex core with decreasing temperature, is directly connected with the low-lying bound states in the vortex core. In addition to the influence of this effect on the *static* vortex structure, this behavior is also important for the *dynamic* vortex properties. In the following, we refer to this as the ‘‘Kramer-Pesch effect.’’ Whereas in the classical superconductors the clean-limit condition, assumed by Kramer and Pesch in their treatment, can hardly be achieved, since the dirty limit is more valid in these materials, in the cuprate superconductors the clean limit often appears to be well established. This clean limit in the cuprates results from the small value of the superconducting coherence length ξ , which is about ten times smaller than in the classical superconductors. Therefore, the issue of the existence or the absence of the Kramer-Pesch effect becomes highly important in the cuprate superconductors. It appears that up to now this subject has hardly been discussed in the literature.

In this paper, we present a brief overview of the spatial structure of a vortex and the influence of low-lying bound states in an isolated vortex core. We also discuss recent experimental results on vortex dynamics obtained for c -axis-oriented epitaxial films or single crystals of various cuprate superconductors in conjunction with the Kramer-Pesch effect.

II. STATIC CASE OF THE KRAMER-PESCH EFFECT

The physics of the vortex core for a classical high- κ superconductor is usually described by the Bardeen-Stephen model.³ This model is valid in the dirty limit when the quasiparticle mean free path l is much shorter than the superconducting coherence length ξ , which limits the radial size of

the vortex core. In the dirty limit, the motion of the quasiparticles gets well randomized within the core. The first calculations of the electronic vortex structure in the clean limit ($l > \xi$) and for $B \ll B_{C2}$ were performed in 1965 by Caroli, de Gennes, and Matricon using the Bogoliubov equations.^{4,5} Subsequently, for $B \ll B_{C2}$ these calculations were extended by Kramer and Pesch using the Eilenberger equations.^{1,2} These authors found that for $T \ll T_c$ in the clean limit the order parameter and supercurrent density increase with the radial distance from the vortex center over a length scale ξ_1 , which is much smaller than the BCS coherence length $\xi_{\text{BCS}} = \hbar v_F / \pi \Delta_{\text{BCS}}$. Here v_F is the quasiparticle Fermi velocity and Δ_{BCS} is the superconducting energy gap. For $T \gg k_B T_c^2 / \epsilon_F \approx \Delta_{\text{BCS}}^2 / k_B \epsilon_F$ (ϵ_F = Fermi energy) and $\kappa \gg 1$, Kramer and Pesch showed that

$$\xi_1 = \xi_{\text{BCS}} \frac{T}{T_c}. \quad (1)$$

As an important consequence of this result, we note that with decreasing temperature the vortex diameter shrinks proportionally to T . Associated with this shrinking of the vortex core is a logarithmic reduction of the density of states at the Fermi surface given by

$$N \approx N_0 2 \pi^3 \xi_{\text{BCS}}^2 / [3 \ln(\xi_{\text{BCS}} / \xi_1)]. \quad (2)$$

Here N_0 is the density of states per unit volume in the normal state. Kramer and Pesch also discussed this behavior in the framework of the Bogoliubov equations, closely following the method of Caroli and co-workers.^{4,5} They could demonstrate that this shrinking of the vortex is connected to the low-lying bound states in the vortex core. The wave functions of these states vary spatially over atomic distances. Only these states with angular momentum quantum number $\mu = \pm(m + 1/2)$ contribute via self-consistency equations to the slope of $|\Delta(r)|$ and $j_s(r)$ in the limit $r \rightarrow 0$ (m = integer; r = quasiparticle distance from the vortex center; j_s = supercurrent density). As shown by Kramer and Pesch, the derivative $d\Delta/dr$ of the order parameter near the vortex center with decreasing temperature increases proportionally to T_c/T . The important length scale for this singularity is the

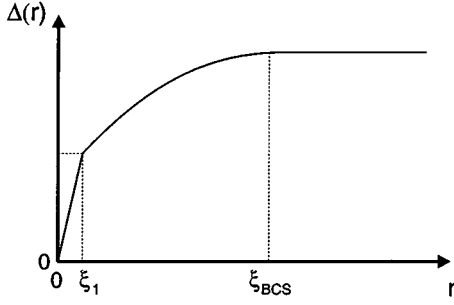


FIG. 1. The two length scales ξ_1 and ξ_{BCS} of the radial vortex size (Ref. 7).

length ξ_1 . However, the total vortex core extends radially up to about the BCS coherence length ξ_{BCS} . This situation is shown schematically in Fig. 1.

The shrinking of the vortex core is associated with the thermal population of the various bound states in the core. Of course, this shrinking process is expected to terminate at some temperature where only the lowest bound state (minigap) remains populated. This lower temperature limit is given by $T \approx k_B T_C^2 / E_F$, and at this temperature, we have $\xi_1 = 1/k_F$ (k_F = Fermi wave number). According to Kramer and Pesch, the exact value of the lowest bound state is given by $\varepsilon_{\text{min}} \approx \Delta_{\text{BCS}}^2 (2\varepsilon_F)^{-1} \ln(\xi_{\text{BCS}}/\xi_1)$ for $T \ll T_C$. The logarithmic factor was missing in the calculations by Caroli *et al.*, due to the assumption $\xi_1 \approx \xi_{\text{BCS}}$. The analytical results found by Kramer and Pesch were numerically confirmed by Gygi and Schlüter.⁶

Recently, Volovik discussed the Kramer-Pesch effect using concepts also appearing in relativistic field theory.^{7,8} He extended the theory also to more complicated vortices, as they arise in unconventional superfluids and superconductors. In the low-energy limit of the quasiparticle spectrum in the core, the mass term of the Bogoliubov-Hamiltonian can be neglected. The massless chiral fermions behave like elementary particles: they obey the Weyl equation like neutrinos or left or right electrons. As a consequence, the energy spectrum of the low-energy fermions becomes relativistic and linear. Thus, in contrast to the situation in particle physics, in this case, the symmetry of the system is enhanced in the *low-energy* limit.⁸

In the semiclassical approximation the energy spectrum of these fermions is characterized by two quantum numbers, the wave number k_z along the vortex axis and the impact parameter $\tilde{y} = r \sin \alpha$, which is the smallest distance for the angular momentum from the vortex axis. Here α is the angle between the quasiparticle trajectory and the radial vector connecting the quasiparticle location and the vortex center. For large distances and impact parameters, we deal with the bulk value of the order parameter. The typical quasiparticle trajectory has a large impact parameter, except for a small cone $\tilde{y} = r \sin \alpha$. This cone represents a set of bound states in the vortex core. Since for small values of the impact parameter the small values of α become most relevant, in the following we approximate $\sin \alpha \approx \alpha$ and write $\tilde{y} = r\alpha$. Similar to the quantum-mechanical case, say, for the central Coulomb potential, where the states with the higher quantum number extend further away from the center of the potential, the

states with the higher impact parameter also have a higher energy and extend further away from the vortex center.

In conventional, singly quantized vortices the energy spectrum then has the following form:

$$\varepsilon(k_z, \tilde{y}) = q\tilde{y} \frac{\Delta^2}{\varepsilon_F}. \quad (3)$$

Here $q\tilde{y} = n_l$ represents the angular momentum quantum number of the bound state. The crossing of zero energy occurs for $\tilde{y} = 0$ for all k_z . This leads to a one-dimensional Fermi surface for the low-lying states. This means that the bound states make up their own Fermi surface, which is a Fermi line in this case. (Of course, this dimensional reduction is associated with the fact, that the two quantum numbers k_x and k_y , representing the quasiparticle state in the absence of a magnetic field, have been contracted into one).

In the following we assume that the minigap is small, $\Delta^2/\varepsilon_F \ll k_B T$. Then, with the quasiclassical approximation one finds

$$k_F(r\alpha) \frac{\Delta^2}{\varepsilon_F} \approx k_B T \quad (4)$$

or

$$\alpha = \frac{1}{r} \left(\frac{k_B T}{k_F(\Delta^2/\varepsilon_F)} \right) \equiv \frac{\xi_1}{r}. \quad (5)$$

In Eq. (5) a new length scale ξ_1 is introduced, characterizing the physical properties of the bound states. This length scale can be written as

$$\xi_1 = \xi_{\text{BCS}} \frac{T}{T_C}. \quad (6)$$

The sharp Fermi function of the chiral fermions has important consequences for the quasiparticle distribution, and the energy becomes a sensitive function of the coordinates of the quasiparticle trajectory.

Volovik discussed in detail the limit $T \ll T_C$, where only the bound states are populated and where the Fermi function is sufficiently narrow and close to a step function. In this case, the length scale ξ_1 becomes smaller than ξ_{BCS} and controls the properties of the vortex core near the origin. As a function of the distance from the vortex center, the order parameter displays a kink and the slope at the origin approaches infinity for $T \rightarrow 0$. With increasing temperature the states with the higher impact parameters become populated.

In conclusion, we note that the bound states which can be thermally populated are responsible for this peculiar behavior of the vortex core. In contrast, for the dirty limit, when reducing the temperature from near T_C to very low values, the changes of the vortex size are only relatively small.⁹

III. DYNAMIC CASE OF THE KRAMER-PESCH EFFECT

One would expect that the considerations for the static case also apply to a moving vortex in the clean limit and for sufficiently low temperatures where only the bound states are excited. Larkin and Ovchinnikov treated this situation and

microscopically calculated the temperature dependence of the electric conductivity at very low temperatures.¹⁰ They obtained for the conductivity σ :

$$\frac{\sigma}{\sigma_n} = 0.23 \frac{B_{C2}}{B} \ln \left(\frac{\Delta_0}{k_B T} \right) \quad (7)$$

(σ_n =conductivity in the normal state). Here the logarithmic term on the right results from the reduction of the vortex size due to the Kramer-Pesch effect. In the absence of the Kramer-Pesch effect, this logarithmic term would be replaced by a number of order unity. Bardeen and Sherman also obtained the expression of Eq. (7) by semiphenomenological calculations, except for a numerical factor of 4/3.¹¹

In the following, we extend these considerations to a vortex moving at high velocities. In contrast to the static case, where the bound states are populated only by an increase in temperature, the generation and energetic excitation of the quasiparticles now can also originate from an increasing electric bias current. Again, in this case, the low-temperature limit must be satisfied such that the quasiparticles are localized in the vortex core. The current-induced quasiparticle excitations only become appreciable at sufficiently high currents. We now deal with an electronic nonequilibrium in the quasiparticle distribution for the low-temperature limit. It is this situation which was treated by Larkin and Ovchinnikov.¹² At sufficiently high currents, the quasiparticle distribution function is not dominated any more by the bath temperature T , but instead by an effective temperature T^* , which is raised above T by the electric field.¹² By analogy, the core diameter now becomes proportional to T^* at very low temperatures. The generation and heating of the quasiparticles in the vortex core is now caused by the electric field. The effective temperature T^* is given by

$$k_B T^* = \Delta \left[k_B T_C \frac{\tau_\varepsilon}{\hbar} \left(\frac{j}{j_C} \right)^2 \right]^{1/5}. \quad (8)$$

Here, τ_ε is the energy relaxation time of the quasiparticles, \hbar is Planck's constant divided by 2π , j is the electric current density, and j_C is the critical pair-breaking current density. The quasiparticle heating is now taken into account by replacing T in Eq. (7) by the effective temperature T^* from Eq. (8). In a sufficiently strong electric field we can have $T^* \gg T$, and the diameter of the vortex core increases proportionally to T^* . Inserting T^* into Eq. (7), we see that the resistivity diverges for $k_B T^* = \Delta$, if we assume the exact validity of Eqs. (7) and (8) up to this point. The quasiparticles within the vortex core are energetically excited to the value of Δ and leave the core region with subsequent recombination and emission of phonons. Denoting the current $I = I^*$, at which $k_B T^* / \Delta = 1$, we obtain from Eq. (8):

$$\frac{I^*}{I_C} = \left[\frac{\hbar}{k_B T_C \tau_\varepsilon} \right]^{1/2}, \quad (9)$$

and the following result for the voltage-current (V - I) characteristic:

$$V = 10.9 \frac{L}{wd} \tilde{\rho} \frac{B}{B_{C2}} \frac{I}{\ln(I^*/I)}. \quad (10)$$

Here L , w , and d are length, width, and thickness of the sample, respectively, and $I_C = j_C wd$. The quantity $\tilde{\rho}$ denotes the resistivity associated with the vortex core. Here we keep in mind that in the cuprate superconductors in general $\tilde{\rho}$ can be smaller than the normal-state resistivity ρ_n . (It is only in the dirty limit where we expect $\tilde{\rho} = \rho_n$.) We see that the V - I characteristic diverges at I^* , and that $I^* \propto (\tau_\varepsilon)^{-1/2}$. The factor $\ln(I^*/I)$ in the denominator of Eq. (10) originates from the Kramer-Pesch effect in close analogy to the influence of the temperature in the logarithmic factor of Eq. (7). If this vortex contraction with decreasing temperature were absent, $\ln(I^*/I)$ would be replaced by a number of order unity.

Regarding the validity of Eqs. (7) and (8) up to $T^* = \Delta/k_B$ we note that this is questionable and that both equations are accurate only in the range of effective temperatures $T^* < \Delta/k_B$.¹³ We will return to this issue below in the discussion of the experimental results.

Summarizing, the Kramer-Pesch effect is due to the population of the bound states in the vortex core in the low-temperature limit. In the static case, this population is achieved by thermal excitation for increasing temperature. In the dynamic case, the excitation due to the current-induced electric field can become dominating.

IV. SPECIAL FEATURES OF THE HIGH- T_C SUPERCONDUCTORS

An important point underlying the Kramer-Pesch effect is the existence of a quasicontinuum of the bound states in the vortex core, so that the calculations can be performed in the quasiclassical limit. In the quasiclassical limit we have $\xi k_F \gg 1$ and the energy of the lowest bound state (minigap) $\Delta^2/\varepsilon_F \propto 1/\xi^2$ is very small. This situation is well established in the classical superconductors. However, in the high- T_C superconductors the situation is quite different, since Δ is larger and ε_F is smaller than in the classical superconductors, (ξ^2 is by about four orders of magnitude smaller than in the classical superconductors). Hence, only a few bound states in the vortex core are expected for the high- T_C superconductors. Recent spectroscopic experiments appear to have confirmed this expectation.^{14,15} In this quantum limit $\xi k_F < 1$ the Kramer-Pesch effect is not expected any more in its standard form.¹⁶ Therefore, the case of a short coherence length must be distinguished from the one with a large coherence length.

A second important point concerns the influence of possibly d -wave symmetry of the order parameter. Presently, there exists an increasing amount of evidence for d -wave symmetry. Recently, Ichioka *et al.* calculated the electronic vortex structure for d -wave symmetry with the Eilenberger formalism finding a strong Kramer-Pesch effect in the static case.¹⁷ However, up to now no calculations for the dynamic case of high vortex velocities regarding the Kramer-Pesch effect and a possible current dependence of the electric resistivity in the presence of d -wave symmetry have been reported. The delocalized quasiparticles from the node lines in the outer regions are likely to play also an important role. For a moving vortex these delocalized quasiparticles contrib-

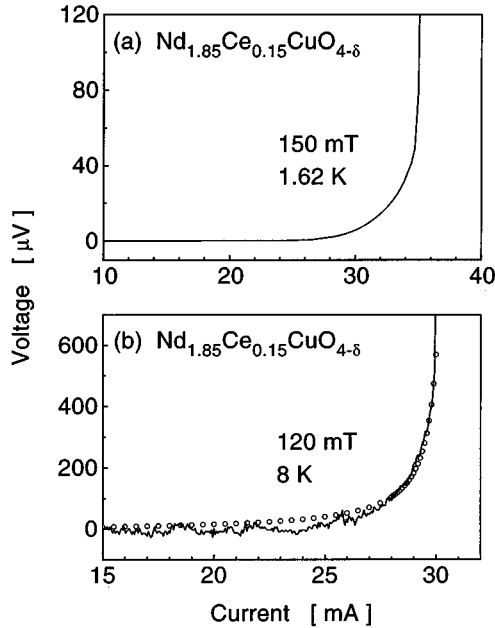


FIG. 2. Voltage vs current for two temperatures and magnetic fields: (a) 1.62 K, 150 mT; (b) 8 K, 120 mT. The recordings are shown only for the higher part of the current range. For comparison, the open circles represent a calculated $V-I$ curve using Eq. (10) and the parameters given in the text.

ute mainly to the dissipation, and the Kramer-Pesch effect may become unobservable in the $V-I$ characteristic.

V. EXPERIMENTS

In the following we discuss recent experimental results for the electric resistance at high vortex velocities and for the microwave power absorption in the mixed state.

A. Resistance at high vortex velocities

Recently, we reported strong indications for the logarithmic singularity in the flux-flow resistance predicted by Larkin and Ovchinnikov for $T \ll T_C$. The experiments were performed for epitaxial c -axis-oriented films of NdCeCuO .¹⁸ This material well satisfies the clean-limit condition. The coherence length in the ab plane is about $\xi_{ab}(0) = 8$ nm (Ref. 19) and is higher than for YBaCuO by a factor of 8. The electron mean free path is in the range $l = 15\text{--}60$ nm.²⁰ For NdCeCuO the temperature dependence of the in-plane magnetic penetration depth²¹ and of the microwave surface impedance^{19,20,21} is consistent with a single-gap s -wave BCS model.

In order to avoid sample heating, we measured the $V-I$ characteristics using a rapid single pulse technique. The instrumentation was the same as in our previous study of YBaCuO .²² For temperatures at and below 4.2 K the sample was in direct contact with liquid He. The bath temperature has been reduced down to below the lambda point $T_\lambda = 2.17$ K. We have investigated four NdCeCuO samples, all showing similar results. In the following we present data for a sample with the following parameters: $T_C = 24$ K, ρ_n (25 K) = $50 \mu\Omega \text{ cm}$, $d = 120$ nm, $w = 20 \mu\text{m}$, and $L = 200 \mu\text{m}$. In Fig. 2 we present two typical curves of the voltage plotted

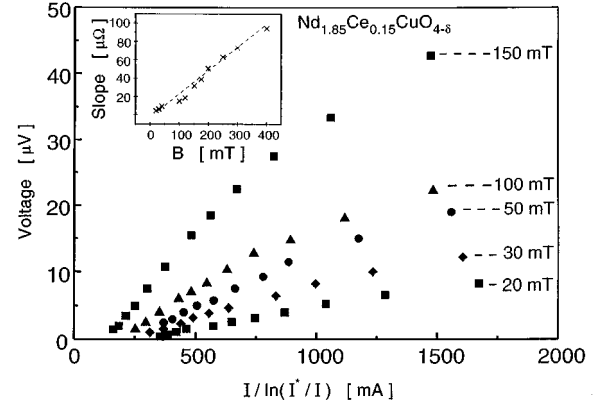


FIG. 3. Voltage vs $I/\ln(I^*/I)$ at $T = 4.2$ K for five magnetic fields as indicated. The inset shows the slope of such curves up to $B = 400$ mT.

versus the current for different temperatures. The highly non-linear behavior expected from the term $\ln(I^*/I)$ in the denominator of Eq. (10) can clearly be seen.

As we have pointed out in Sec. III, the exact validity of Eqs. (7)–(10) is expected only in the effective temperature range $T^* < \Delta/k_B$.¹³ This is analogous to the static case where we are restricted to the low-temperature regime such that only the low-lying states in the vortex core are excited. Therefore, in the dynamic case we have to concentrate on the lower end of the applied transport current. Hence, we have treated I^* as an adjustable parameter, which we have varied until the voltage plotted versus the normalized current $I/\ln(I^*/I)$ yielded a straight line in the lower current range. A typical result is presented in Fig. 3, where such plots are shown for five values of the magnetic flux density B at $T = 4.2$ K. The values of the parameter I^* yielding straight lines near the lower current end were about 5% larger than the observed current values I_{sing} , where the voltage starts to diverge. From Eq. (10) the slope of the straight lines is expected to increase proportionally to B . This is also well confirmed by our data, as can be seen in more detail in the inset of Fig. 3. On the other hand, from Fig. 3 we also note that near the upper current end appreciable deviations from the straight lines appear, indicating that here we exceed the range of exact validity of Eqs. (7)–(10).

As we can see from Eq. (9), the quasiparticle energy relaxation time τ_e can be found from the values of the parameter I^* . Taking the values of I^* adjusted for yielding straight lines in plots such as shown in Fig. 3, we obtain the values $\tau_e^{-1} = 1.67 \times 10^9 \text{ s}^{-1}$ for $T = 4.2$ K and $\tau_e^{-1} = 1.72 \times 10^9 \text{ s}^{-1}$ for $T = 1.62$ K. These small values indicate that the quasiparticle energy relaxation rate is strongly suppressed below T_C , similar to our previous results on YBaCuO films.²² Since the Larkin-Ovchinnikov theory¹² applies to the limit of low magnetic fields, in our analysis we have used the values of I^* obtained by extrapolation to $B = 0$. Additional details can be found in Ref. 18.

Our results presented in Figs. 2 and 3 appear to confirm the contraction of the vortex core predicted by Kramer and Pesch. However, this interpretation of our data requires a discussion of a possible influence of Joule heating and/or flux pinning. Turning first to heating effects, we found that no appreciable change in the $V-I$ characteristic could be de-

ected by passing the bath temperature through the λ point. From this it appears that the strong increase of the heat-transfer coefficient during passing into the superfluid state of liquid He did not affect the sample temperature. We thus conclude that the rise of the sample temperature due to Joule heating was negligible.

Turning next to the possible influence of flux pinning, we checked this as follows. Trying to fit our measured highly nonlinear V - I curves such as shown in Fig. 2 by the functional dependence $V \propto I^n$, we found that we need exceptionally high values of the exponent n in the range $n=60$ – 150 . Furthermore, the good fit of the data in Fig. 3 by the straight lines strongly supports the mechanism underlying Eq. (10) instead of flux pinning. For comparison, in Fig. 2(b) we also present a curve (open circles) fitted to the experimental trace (solid line) using Eq. (10) and the following parameters: $\tilde{\rho} = 1.76 \times 10^{-3} \mu\Omega \text{ cm}$, $B/B_{c2} = 1.5 \times 10^{-2}$, $I^* = 30 \text{ mA}$. The value of the core resistivity $\tilde{\rho}$ at $T=8 \text{ K}$ is strongly reduced below the normal-state resistivity $\rho_n(25 \text{ K}) = 50 \mu\Omega \text{ cm}$ near T_C , and correspondingly, the damping coefficient is enhanced. Apparently, the quasiparticle scattering rate τ^{-1} strongly decreases with decreasing temperature below T_C . Such behavior has also been concluded recently from microwave absorption experiments in the mixed state of YBaCuO single crystals²³ and from microwave surface resistance measurements of YBaCuO samples in zero magnetic field.^{24,25}

Following our measurements with the NdCeCuO films, it was interesting also to examine another cuprate material possibly showing d -wave symmetry or strong anisotropy of the order parameter. An additional requirement for this other material was that flux-flow experiments should be possible in the low-temperature limit, i.e., flux pinning should be overcome at sufficiently high current densities. LaSrCuO appeared to fulfill both requirements. For this material there are experimental indications for an unconventional pairing mechanism and node lines of the order parameter. The experimental data from neutron scattering^{26,27} as well as from Raman spectroscopy^{28,29} point to a strongly anisotropic energy gap. The epitaxial c -axis-oriented LaSrCuO films were deposited on single-crystalline SrTiO₃ substrates by laser ablation. Microfabrication of the four-point sample geometry was performed by standard photolithography. For attaching the current and voltage leads, silver pads as large as $2 \times 2 \text{ mm}^2$ were placed on top of the superconducting film, in this way minimizing sample heating due to the contact resistance. The film thickness was 60–100 nm. The length and width of the microbridge was typically 150 and 15 μm , respectively. The superconducting transition temperature was $T_C = 26.5 \text{ K}$. Close to T_C the resistivity was $\rho_n(27 \text{ K}) = 220 \mu\Omega \text{ cm}$. In order to minimize heating effects from power dissipation in the sample, we have performed the measurements in superfluid helium at a bath temperature of 1.52 K. The V - I characteristics were quite different from those for NdCeCuO such as shown in Fig. 2. A typical case is shown in Fig. 4. The curves showed a distinct kink similar to that we have observed earlier for YBaCuO (Ref. 22) indicating an electronic instability at a critical vortex velocity. Near this instability the Joule power dissipation in the sample corresponded to about 10 W/cm^2 . With a heat-transfer coefficient of about $\alpha_t \approx 10 \text{ W/cm}^2 \text{ K}$,^{30,31} the temperature rise of the sample is estimated to about 1 K. This distinct difference we have

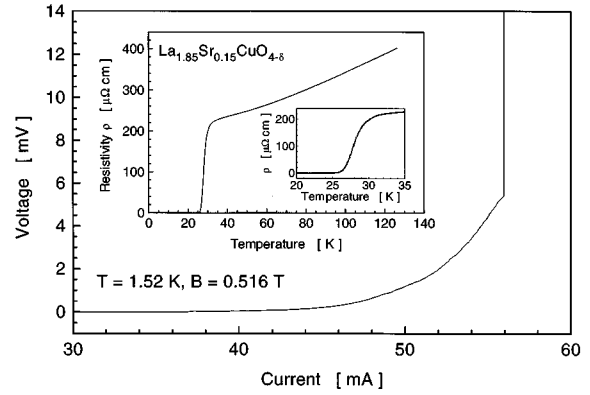


FIG. 4. Voltage vs current for a $\text{La}_{1.85}\text{Sr}_{0.15}\text{CuO}_{4-\delta}$ sample. $T=1.52 \text{ K}$; $B=0.516 \text{ T}$. The inset shows the resistive transition.

found in the resistive behavior between NdCeCuO and LaSrCuO for $T \ll T_C$ strongly suggests that it is the delocalization of the quasiparticles in LaSrCuO due to the strong anisotropy of the energy gap which eliminates the logarithmic dependence of the voltage on the current as expressed in Eq. (10). Apparently, the Kramer-Pesch effect can only be observed if the dissipation is located in the inner vortex core. On the other hand, if the dissipation is dominated from the outer regions surrounding the inner vortex core, the Kramer-Pesch effect remains unobservable via measurements of the dissipation. It seems that this second case is realized in LaSrCuO.

B. Microwave power absorption

For YBaCuO films with a critical temperature of 60 or 90 K flux-flow resistance measurements are highly difficult because of flux pinning. In the following we discuss experiments by Matsuda *et al.*, who measured the microwave power absorption in the mixed state of single crystals of 60 and 90 K YBaCuO using a bolometric technique.²³ The static magnetic field was applied parallel to the c axis. Due to the high-frequency field oriented parallel to the ab plane, the vortices oscillate within their pinning potential. Matsuda, *et al.* were able to measure the microwave power absorption in the temperature range from 30 down to 2.7 K with a resolution of about 0.1 nW. They determined the surface impedance in their samples as a function of the static magnetic field up to 7 T. From their results they obtained the viscous damping coefficient η for vortex motion.

According to Coffey and Clem³² in the low-field regime the surface impedance is given by

$$R_S(B) - R_S(0) = \frac{B\varphi_0}{2\lambda\eta}. \quad (11)$$

The damping coefficient η must now be taken for the proper regime of quasiparticle scattering. Kopnin and Kravtsov³³ calculated the electrical conductivity and the Hall effect in the mixed state of clean type-II superconductors at low temperatures ($k_B T \ll \Delta$) in the regime $\hbar/\tau \ll \Delta$ (τ =quasiparticle scattering time). They pointed out the importance of the level spacing Δ^2/ε_F of the low-lying bound states in the vortex core: in the limit $(\pi/\hbar)(\Delta^2/\varepsilon_F) \ll 1$ we have viscous vortex flow and in the limit $(\pi/\hbar)(\Delta^2/\varepsilon_F) \gg 1$ nondis-

sipative vortex flow. In the former case the Hall angle is small, whereas in the latter case it is large. In the case of a finite Hall angle the damping force appearing in the vortex dynamics consists of two components $\eta v_\varphi + \alpha_H(v_\varphi \times e_z)$, where v_φ is the vortex velocity, e_z a unit vector in the direction of the applied magnetic field, η is the viscous drag coefficient, and α_H is the Hall drag coefficient. The coefficient describing the dissipation [and appearing in Eq. (11)] now consists of the effective coefficient $\eta_{\text{eff}} = (\eta^2 + \alpha_H^2)/\eta$.^{23,33} The Hall angle Θ_H is given by $\tan \Theta_H = \alpha_H/\eta$. In the case of a large Hall angle ($\alpha_H/\eta \gg 1$) one finds^{23,33}

$$\eta_{\text{eff}} = \frac{\alpha_H^2}{\eta} = 0.30 B_{C2} \varphi_0 \frac{1}{\bar{\rho}} \ln\left(\frac{\Delta}{k_B T}\right). \quad (12)$$

It is this expression for η_{eff} , invoking the superclean limit, which has been used by Matsuda, *et al.*²³ for analyzing their data. We note that the factor $\ln(\Delta/k_B T)$ on the right-hand side of Eq. (12) is due to the vortex contraction at low temperatures from the Kramer-Pesch effect. Inserting Eq. (12) into Eq. (11) we obtain the derivative

$$\frac{dB}{dR_S(B)} = 0.60 \lambda B_{C2} \frac{1}{\bar{\rho}} \ln\left(\frac{\Delta}{k_B T}\right). \quad (13)$$

Larkin and Ovchinnikov¹⁰ also treated theoretically the conductivity in the mixed state at low temperatures. However, they only considered the quasiparticle scattering regime $\Delta^2/\varepsilon_F \ll \hbar/\tau \ll \Delta$, where the Hall effect remains negligible. For the damping coefficient η they obtained

$$\eta = 0.23 B_{C2} \varphi_0 \frac{1}{\bar{\rho}} \ln\left(\frac{\Delta}{k_B T}\right). \quad (14)$$

Again, the factor $\ln(\Delta/k_B T)$ on the rhs results from the Kramer-Pesch effect. It is interesting that the numerical values of the damping coefficient in Eqs. (12) and (14) are highly similar. Inserting Eq. (14) into Eq. (11) yields the derivative

$$\frac{dB}{dR_S(B)} = 0.46 \lambda B_{C2} \frac{1}{\bar{\rho}} \ln\left(\frac{\Delta}{k_B T}\right). \quad (15)$$

Using Fig. 3 of Ref. 23 we have obtained the values of the derivative dB/dR_S for the 60 K YBaCuO sample in the low-field limit. These values are plotted in Fig. 5 versus $\ln(T_C/T)$. As expected from Eqs. (13) and (15), the data well fit a straight line with the slope $dB/dR_S = 235T/\Omega$.³⁴ Here we emphasize that in the relevant low-temperature regime the magnetic penetration depth λ (Ref. 35) as well as B_{C2} and $\bar{\rho}$ are nearly independent of temperature. Noting that the logarithmic factor in Eqs. (13) and (15) originates from the contraction of the vortex core due to the Kramer-Pesch effect, we conclude that the data of Matsuda *et al.* clearly display this effect for 60 K YBaCuO.

To check whether the slope of the straight line in Fig. 5 looks reasonable, we calculated the core resistivity $\bar{\rho}$ from this slope in combination with Eq. (15). Taking the values $\lambda = 140$ nm (Ref. 35) and $B_{C2} = 90$ T we find $\bar{\rho} = 4.7 \mu\Omega$ cm. Using Eq. (13) instead of Eq. (15) yields nearly the same result. In view of the fact that below T_C a strong reduction of the quasiparticle scattering rate with decreasing temperature

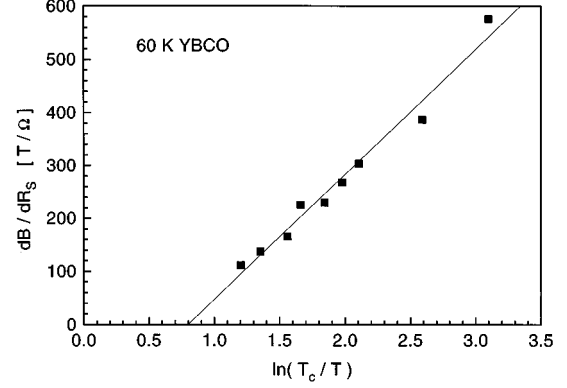


FIG. 5. dB/dR_S vs $\ln(T_C/T)$. The values were taken from Fig. 3 of Ref. 23.

has generally been found in the cuprates, this value of $\bar{\rho}$ appears reasonable. Matsuda *et al.* have also reported such a strongly reduced value of $\bar{\rho}$ for $T \ll T_C$.²³

VI. DISCUSSION AND CONCLUSIONS

Whereas for 60 K YBaCuO the microwave absorption data of Matsuda *et al.*²³ clearly show the influence of the factor $\ln(\Delta/k_B T)$ in Eqs. (13) and (15) arising from the Kramer-Pesch effect, for 90 K YBaCuO they observed a temperature-independent derivative dB/dR_S in the low-field limit, as displayed in Fig. 4 of Ref. 23. This strongly suggests that in 90 K YBaCuO the Kramer-Pesch effect is absent. As has been discussed in detail by Golosovsky, Tsindlekt, and Davidov,³⁶ the dominant number of high-frequency experiments dealing with vortex dynamics indicate that for 60 and 90 K YBaCuO the damping coefficient of the vortex motion is consistent with the predictions for the clean limit. However, for low temperatures, in 60 K YBaCuO the damping coefficient suggests a transition into the superclean limit. The vortex contraction with decreasing temperature due to the Kramer-Pesch effect results in an increasing level spacing between the bound states in the vortex core and, therefore, in a decreasing phase space for quasiparticle scattering. Hence, it seems possible that in 60 K YBaCuO for low temperatures the superclean limit is at least partly a result of the vortex contraction due to the Kramer-Pesch effect. This concept is also supported by the fact that 60 K YBaCuO displays a large Hall angle (in contrast to 90 K YBaCuO, where the Kramer-Pesch effect is absent).³⁴

For 90 K YBaCuO the coherence length is smaller than for 60 K YBaCuO,³⁷ and we may approach already the quantum limit, where the core region of the vortex is empty of the low-energy excitations. However, in this context a discussion of the influence of the symmetry of the order parameter becomes necessary. For 90 K YBaCuO there exists a large amount of evidence that the order parameter shows *d*-wave symmetry.^{38,39} For 60 K YBaCuO recent phase-sensitive tunneling experiments suggest that the symmetry is not *s* wave.⁴⁰ The calculations by Ichioka *et al.*,¹⁷ indicating a strong Kramer-Pesch effect also in the case of an order parameter with *d*-wave symmetry, appear to be consistent with our conclusions given above. The absence of the Kramer-Pesch effect for 90 K YBaCuO (with its very small coher-

ence length) may be explained in terms of the dominant role of the regions outside the inner vortex core in the dissipation process. In contrast to this, for 60 K YBaCuO the inner vortex core appears to play still a significant role.

In this context we emphasize that our discussion in Sec. V A demonstrated the Kramer-Pesch effect for NdCeCuO which shows *s*-wave symmetry of the order parameter and which has a coherence length eight times larger than 90 K YBaCuO.¹⁹

ACKNOWLEDGMENTS

This work was supported by the Deutsche Forschungsgemeinschaft. S.G.D. also obtained financial support from the Studienstiftung Gerhard Rösch. The authors thank Yu. N. Ovchinnikov, N. Schopohl, G. E. Volovik, and Y. Yip for very valuable discussions. They also thank B. Mayer and J. Mannhart for the preparation of the LaSrCuO samples, and M. P. Risse for technical support.

-
- ¹L. Kramer and W. Pesch, *Z. Phys.* **269**, 59 (1974).
²W. Pesch and L. Kramer, *J. Low Temp. Phys.* **15**, 367 (1973).
³J. Bardeen and M. J. Stephen, *Phys. Rev.* **140**, A1197 (1965).
⁴C. Caroli, P. G. De Gennes, and J. Matricon, *Phys. Lett.* **9**, 307 (1964).
⁵C. Caroli and J. Matricon, *Phys. Kondens. Mater.* **3**, 380 (1965).
⁶F. Gygi and M. Schlüter, *Phys. Rev. B* **43**, 7609 (1991).
⁷G. E. Volovik, *Pis'ma Zh. Eksp. Teor. Fiz.* **58**, 455 (1993).
⁸G. E. Volovik, *Exotic Properties of Superfluid ³He* (World Scientific, Singapore, 1992).
⁹L. Kramer, W. Pesch, and R. J. Watts-Tobin, *J. Low Temp. Phys.* **14**, 29 (1974).
¹⁰A. I. Larkin and Yu. N. Ovchinnikov, *Zh. Eksp. Teor. Fiz.* **23**, 210 (1976) [*JETP Lett.* **23**, 187 (1976)].
¹¹J. Bardeen and R. D. Sherman, *Phys. Rev. B* **12**, 2634 (1975).
¹²A. I. Larkin and Yu. N. Ovchinnikov, *Zh. Eksp. Teor. Fiz.* **73**, 299 (1977) [*Sov. Phys. JETP* **46**, 155 (1977)].
¹³G. E. Volovik (private communication).
¹⁴K. Karrai, E. J. Choi, F. Dumore, S. Liu, H. D. Drew, Qi Li, D. B. Fenner, Y. D. Zhu, and F. C. Zhang, *Phys. Rev. Lett.* **69**, 152 (1992).
¹⁵I. Maggio-Aprile, Ch. Renner, A. Erb, E. Walker, and Ø. Fischer, *Phys. Rev. Lett.* **75**, 2754 (1995).
¹⁶N. Schopohl (private communication).
¹⁷M. Ichioka, N. Hayashi, N. Enomoto, and K. Machida, *Phys. Rev. B* **53**, 15 316 (1996).
¹⁸S. G. Doettinger, S. Anders, R. P. Huebener, H. Haensel, and Yu. N. Ovchinnikov, *Europhys. Lett.* **30**, 549 (1995).
¹⁹S. M. Anlage, D. Wu, J. Mao, X. X. Xi, T. Venkatesan, J. L. Peng, and R. L. Greene, *Phys. Rev. B* **50**, 523 (1994).
²⁰D. H. Wu, J. Mao, S. N. Mao, J. L. Peng, X. X. Xi, T. Venkatesan, R. L. Greene, and S. M. Anlage, *Phys. Rev. Lett.* **70**, 85 (1993).
²¹C. W. Schneider, Z. H. Barber, J. E. Evetts, S. N. Mao, X. X. Xi, and T. Venkatesan, *Physica C* **233**, 77 (1994).
²²S. G. Doettinger, R. P. Huebener, R. Gerdemann, A. Kühle, S. Anders, T. G. Traeuble, and J. C. Villegier, *Phys. Rev. Lett.* **73**, 1691 (1994).
²³Y. Matsuda, N. P. Ong, Y. F. Yan, J. M. Harris, and J. B. Peterson, *Phys. Rev. B* **49**, 4380 (1994).
²⁴D. A. Bonn, R. Liang, T. M. Riseman, D. J. Baar, and D. C. Morgan, *Phys. Rev. B* **47**, 11 314 (1993).
²⁵D. C. Morgan, Kuan Zhang, D. A. Bonn, Ruixing Liang, W. N. Hardy, C. Kallin, and A. J. Berlinsky, *Physica C* **235**, 2015 (1994).
²⁶K. Yamada, S. Wakimoto, G. Shirane, C. H. Lee, M. A. Kastner, S. Hosoya, M. Greven, Y. Endah, and R. J. Birgeneau (unpublished).
²⁷J. Rossat-Mignod, L. P. Regnault, P. Bourges, C. Vettier, P. Barlet, and J. Y. Henry, *Physica B* **49**, 15 305 (1994).
²⁸J. C. Irwin, X. K. Chen, H. J. Trodahl, T. Kimura, and K. Kishio, *J. Supercond.* (to be published).
²⁹K. Chen, J. C. Irwin, H. J. Trodahl, T. Kimura, and K. Kishio, *Phys. Rev. Lett.* **73**, 3290 (1994).
³⁰H.-J. Schulze and K. Keck, *Appl. Phys. A* **34**, 243 (1984).
³¹W. J. Skocpol, M. R. Beaseley, and M. Tinkham, *J. Appl. Phys.* **45**, 4054 (1974).
³²M. W. Coffey and J. R. Clem, *Phys. Rev. Lett.* **67**, 386 (1991).
³³N. B. Kopnin and V. E. Kravtsov, *Pis'ma Zh. Eksp. Teor. Fiz.* **23**, 631 (1976).
³⁴S. G. Doettinger, Ph.D. thesis, University of Tuebingen, 1996.
³⁵H. E. Porteanu, K. Karrai, R. Seifert, F. Koch, P. Berberich, and H. Kinder, *Phys. Rev. Lett.* **75**, 3934 (1995).
³⁶M. Golosovsky, M. Tsindlekht, and D. Davidov, *Supercond. Sci. Technol.* **9**, 1 (1996).
³⁷K. G. Vandervoort, U. Welp, J. E. Kessler, H. Claus, G. W. Crabtree, W. K. Kwok, A. Umezawa, B. W. Veal, J. W. Downey, and A. P. Paulikas, *Phys. Rev. B* **43**, 13 042 (1991).
³⁸C. C. Tsuei, J. R. Kirtley, C. C. Chi, Lock See Yu-Jahnes, A. Gupta, T. Shaw, J. Z. Sun, and M. B. Ketchen, *Phys. Rev. Lett.* **73**, 593 (1994).
³⁹J. R. Kirtley, C. C. Tsuei, J. Z. Sun, C. C. Chi, Lock See Yu-Jahnes, A. Gupta, M. Rupp, and M. B. Ketchen, *Nature (London)* **373**, 225 (1995).
⁴⁰D. A. Brawner and H. R. Ott, *Phys. Rev. B* **53**, 8249 (1996).